into $PH_3 + H_2$, in spite of its relatively large barrier for a unimolecular decomposition.

It may even be that another PH_5 may take the role of the Lewis acid.

In fact we find (see Table I) that the hydride affinity, i.e., the energy gain in the reaction $PH_5 + H^- \rightarrow PH_6^-$, is ~34 kcal/mol, which can be compared with the hydride affinities of H_2CO, 27 kcal/mol,[27] or BH_3, 65 kcal/mol.[26] So PH_5 is a moderate Lewis acid, which is also illustrated by the relatively small endoergicity of ~130 kcal/mol of the reaction $2PH_5 \rightarrow PH_4^+ + PH_6^-$. We conclude that the presence of another PH_5 molecule may lower the barrier for the zwitterionic desintegration considerably, but we hesitate to confirm this by explicit calculations.

As to the preparation of PH_5 one has to meet two basic difficulties. Starting from $PH_3 + H_2$ one has to overcome a barrier of ~80 kcal/mol, which is quite hopeless. Starting from $PH_4^+ + H^-$ one should get more easily $PH_3 + H_2$ than PH_5.

Concerning the reaction $PX_5 \rightarrow PX_3 + X_2$ one notes that this reaction is endoergic for X = Cl; one should hence rather consider the reverse reaction. Taking the difference in the sign of the reaction energy into account one should expect a potential hypersurface with a similar qualitative feature, i.e., a flat saddle region with a competition but not a clear distinction of a concerted and a zwitterionic process.

The first reaction step for the addition of Cl_2 to PCl_3 should be easier than that for the addition of H_2 to PH_3 since the antibonding σ^* MO of Cl_2 is much lower in energy such that Cl_2 is more ready to accept charge. This should lower the barrier for both the concerted and the zwitterionic process, but it is hard to predict by simple qualitative arguments which of the two will be lower.

Acknowledgment. One of the authors (Jan Wasilewski) thanks the Alexander-von-Humboldt foundation for a research fellowship that enabled him to start this investigation and to participate in accomplishing it. The computations were partly done on the Telefunken TR 440 of the computer center of the Ruhr-Universität Bochum, but mainly on the INTERDATA (Perkin-Elmer) 8/32 "minicomputer". Helpful discussions with Dr. H. Kollmar and Dr. V. Staemmler are gratefully acknowledged.

(26) C. Hoheisel and W. Kutzelnigg, *J. Am. Chem. Soc.*, **97**, 6970 (1975).
(27) H. Kollmar, private communication.

Registry No. PH_5, 13769-19-2; PH_3, 7803-51-2; H_2, 1333-74-0; PH_6^-, 79839-88-6; PH_4, 25530-87-4; PH_4^+, 16749-13-6.

Concerted Dihydrogen Exchange between Ethane and Ethylene. SCF and FORS Calculations of the Barrier

David F. Feller, Michael W. Schmidt, and Klaus Ruedenberg*

Contribution from the Ames Laboratory[1] and Department of Chemistry, Iowa State University, Ames, Iowa 50011. *Received May 22, 1981*

Abstract: The concerted dihydrogen exchange reaction between eclipsed ethane and ethylene yielding ethylene and ethane is "symmetry allowed". Nonetheless, on the basis of SCF and full optimized reaction space (FORS) MCSCF calculations, a reaction barrier of about 71 kcal/mol is predicted. The electronic rearrangements and the origin of the barrier are analyzed.

The least-motion concerted transfer of two hydrogen atoms from eclipsed ethane to ethylene is symmetry allowed and has been explicitly discussed as a paradigm by Woodward and Hoffman[2a] and by Goddard.[2b] Rye and Hansen[3a] have conjectured such a process to play an intermediary role in the hydrogenation of ethylene over a metal catalyst, supposing that the adsorbed ethylene might have a structure similar to that of ethane. Doering and Rosenthal[3b] have observed dihydrogen exchange from *cis*-9,10-dihydronaphthalene to various olefins. The analogous hydrogenation of olefins by diimide[4-6] has long been recognized for its versatility and stereospecificity.

Nontheless, the theoretical investigation reported here reveals the existence of a substantial barrier for the concerted exchange of hydrogens from ethane to ethylene.

In agreement with the reasoning by Woodward and Hoffman[1a] we assume a concerted movement of both hydrogens, maintaining C_{2v} symmetry throughout. We further assume that the activated complex of highest energy occurs for the transition state with D_{2h} symmetry shown in Figure 1 and verify afterward that this geometry is indeed a saddle point on the energy surface.

In the present case, the "conservation of symmetry" is equivalent to the statement that a single-determinant Hartree–Fock SCF wave function can be used to represent the system at all stages of the reaction in the sense that the occupied MO's of the reactants deform continuously and smoothly into the occupied MO's of the products. Accordingly, we first performed ab initio calculations at the SCF level for the reactant/product geometry and for the transition-state geometry. Subsequently we tested the validity of this approximation and, hence, the applicability of the concept of symmetry allowedness by carrying out full optimized reaction space (FORS) multiconfiguration SCF (MCSCF) calculations which allow for the dominant electron correlation effects on the calculated barrier. They also deepen the understanding of the electronic rearrangements.

Method of Calculation

Glossary. The following terms and abbreviations will be used in the sequel.

PAO, primitive atomic orbital: an exponential or a Gaussian multiplied by powers of x, y, and z or by a solid spherical har-

(1) Operated for the U.S. Department of Energy by Iowa State University under Contract No. W-7405-Eng-82. This research was supported by the Director for Energy Research, Office of Basic Energy Science.
(2) (a) Woodward, R. B.; Hoffman, R. "The Conservation of Orbital Symmetry"; Verlag Chemie: Weinheim, 1971; pp 141-144. (b) Goddard, W. A. *J. Am. Chem. Soc.* **1972**, *94*, 793-807.
(3) (a) Rye, R. R.; Hansen, R. S. *J. Phys. Chem.* **1969**, *73*, 1667-1673. (b) Doering, W. von E.; Rosenthal, J. W. *J. Am. Chem. Soc.* **1967**, *89*, 4534-4535.
(4) Miller, C. E. *J. Chem. Educ.* **1965**, *42*, 254-259.
(5) Hunig, S.; Muller, H. R.; Thier, W. *Angew. Chem., Int. Ed. Engl.* **1965**, *4*, 271-280.
(6) (a) Vidyarthi, S. K.; Willis, C.; Back, R. A.; McKitrick, R. M. *J. Am. Chem. Soc.* **1974**, *96*, 7647-7650. (b) Willis, C.; Back, R. A.; Parsons, J. M.; Purdon, J. G. *J. Am. Chem. Soc.* **1977**, *99*, 4451-4456.

0002-7863/82/1504-0960$01.25/0 © 1982 American Chemical Society

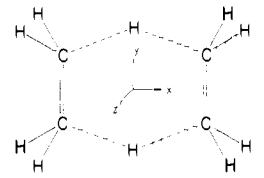

Figure 1. D_{2h} transition state for the reaction $C_2H_6 + C_2H_4 \rightarrow C_2H_4 + C_2H_6$.

monic; in the present work, even-tempered Cartesian Gaussian AO's.[7]

QBO, quantitative basis orbital: a fixed linear combination ("contraction") of PAO's. The QBO's serve as the basis for expanding the MO's. In the present work the QBO's are general, unsegmented, Raffenetti-type contractions of even-tempered PAO's.[8]

SAAP, spin adapted antisymmetrized product: a configuration constructed as an antisymmetrized product of MO's and spin eigenfunctions. The MO's are linear combinations (to be optimized) of QBO's.

FORS, full optimized reaction space: a configuration space spanned by specific SAAP's which are MCSCF optimized. A full configuration space is chosen so as to be invariant under orthogonal transformations among the core MO's and under orthogonal transformations among the reaction MO's.

Occupied MO's or configuration generating MO's: MO's which are used to construct FORS SAAP's.

Core MO's or inactive MO's: occupied MO's whose occupation numbers have the value 2.

Reaction MO's or active MO's: occupied MO's whose occupation numbers have a value less than 2 (but of course larger than zero).

Unoccupied MO's or virtual MO's: those linear combinations of QBO's which are orthogonal to the occupied MO's and, hence, have zero occupation numbers.

Quantitative Basis Orbitals (QBO's). Three different basis sets were used during this investigation. The geometry optimization of the complex was performed with the smallest basis, denoted basis A, consisting of a C(6s/3p), H(3s) set[7] of even-tempered Gaussian PAO's, with the hydrogen functions scaled by the factor 1.1, generally contracted in Raffenetti-style[8b] to an unsegmented C(4s/2p), H(2s) set of QBO's. Once the optimal geometry was found, larger bases were employed. Basis B, of double-ζ quality, contained an increased number of primitives, namely, a C(10s/5p), H(4s) set of PAO's,[7] with the hydrogen unscaled, generally contracted to an unsegmented C(3s/2p), H(2s) set of QBO's. Basis C, of double-ζ plus polarization quality, contains basis B and a set of d functions on carbon and p functions on the reacting hydrogens, with exponents $\zeta_d = 0.75$ and $\zeta_p = 1.0$.[9] This final basis contains 170 PAO's and 86 QBO's.

The Hartree–Fock SCF calculations on ethane, ethylene, and the intermediate complex were performed by using all three bases. The full optimized reaction space (FORS) MCSCF calculations were undertaken with basis B.

FORS Model. The full optimized reaction space (FORS) model was developed to account for the dominant portion of the electron correlation energy changes which occur during a chemical reaction. A FORS wave function consists of *all* the spin adapted antisymmetrized products (SAAP's) consistent with the overall electronic symmetry which can be formed by distributing the electrons involved in the reaction *over all reacting molecular orbitals in all possible ways and with all possible spin couplings.* MCSCF calculations with the dominant SAAP's, selected by a natural orbital analysis of the full CI wave function, are used to determine optimal molecular orbitals, while full CI calculations determine the total FORS wave function and energy. The FORS method and various applications are described in greater detail elsewhere.[10-14]

Table I. Optimal Geometry of D_{2h} Ethane–Ethylene Complex

atoms	x^a	y^a	z^a
C	±2.555	±1.341	0
H(reacting)	0	±1.878	0
H(peripheral)	±3.095	±2.315	±1.729

[a] Coordinates of atoms in units of bohrs (1 bohr = 0.5292 Å) and referring to the coordinate system shown in Figure 1.

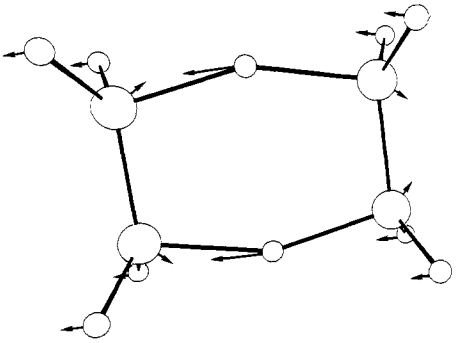

Figure 2. The normal mode (b_{3u}) corresponding to a displacement along the reaction coordinate at the transition state.

Molecular Programs. All calculations, except the normal mode analysis, were performed by using the ALIS system[15] for quantum chemical molecular calculations. The calculation of the normal modes and their frequencies was done by using the GAMESS system,[16] with a standard 3-21G basis.[17]

Results and Discussion of SCF Calculations

Geometry. The determination of the transition state of the reaction considered here is greatly simplified by the fact that it has D_{2h} symmetry. Using basis A, *all geometric parameters of the activated complex were optimized within this symmetry* by SCF calculations. The optimal geometry is presented in Table I. The CC bonds of the complex are intermediate in length (1.42 Å) between ethylene (1.33 Å) and ethane (1.57Å). The four central CH bonds are quite long (1.38 Å), but the peripheral CH bonds remain at 1.09 Å. The peripheral hydrogens are bent back 29.0°, again intermediate between ethylene (0°) and ethane (51.3°).

That this optimized geometry of the intermediate complex is indeed a saddle point on the molecular energy hypersurface was verified by calculating all normal modes and their frequencies. Diagonalization of the mass weighted Hessian matrix yielded exactly one negative force constant which is the condition for a transition state. The corresponding imaginary frequency was found

(7) Schmidt, M. W.; Ruedenberg, K. *J. Chem. Phys.* **1979**, *71*, 3951–3962.
(8) (a) Bardo, R. D.; Ruedenberg, K. *J. Chem. Phys.* **1974**, *60*, 918–931. (b) Raffenetti, R. C. *J. Chem. Phys.* **1973**, *58*, 4452–4458.
(9) Dunning, T. H.; Hay, P. J. "Methods of Electronic Structure Theory"; Schaefer, H. F., Ed.; Plenum Press: New York, 1977; pp 1–27.
(10) Ruedenberg, K.; Sundberg, K. R. "Quantum Science"; Calais, J. L., Goscinski, O., Linderberg, J., Öhrn, Y., Eds.; Plenum Press: New York, 1976; pp 505–515.
(11) (a) Ruedenberg, K. "Post Hartree-Fock: Configuration Interaction"; Lawrence Berkeley Laboratory: University of California, 1979; pp 46–64. (b) Ruedenberg, K. "Report on 1980 NRCC Workshop on MCSCF Methods"; Lawrence Berkeley Laboratory: University of California, in press.
(12) (a) Cheung, L. M.; Sundberg, K. R.; Ruedenberg, K. *Int. J. Quantum Chem.* **1979**, *16*, 1103–1139. (b) Cheung, L. M.; Sundberg, K. R.; Ruedenberg, K. *J. Am. Chem. Soc.* **1979**, *100*, 8024–8025.
(13) Ruedenberg, K.; Schmidt, M. W.; Gilbert, M. *Proc. Natl. Acad. Sci. U.S.A.*, in press.
(14) Johnson, R. P.; Schmidt, M. W. *J. Am. Chem. Soc.* **1981**, *103*, 3244–3249.
(15) Elbert, S. T.; Cheung, L. M.; Ruedenberg, K. NRCC Software Catalog, Vol. 1, Program No. QM01 (ALIS), 1980. The ALIS (Ames Laboratory-Iowa State University) program system is part of the National Resource for Computations in Chemistry program library. It contains a version of the BIGGMOL1 integral program[8b] and a MCSCF program based on the method described in: Ruedenberg, K.; Cheung, L. M.; Elbert, S. T. *Int. J. Quantum Chem.* **1979**, *16*, 1069–1101.
(16) Dupuis, M.; Spangler, D.; Wendoloski, J. J. NRCC Software Catalog, Vol. 1, Program No. QG01 (GAMESS), 1980. GAMESS is an acronym for General Atomic and Molecular Electronic Structure System.
(17) Binkley, J. S.; Pople, J. A.; Hehre, W. J. *J. Am. Chem. Soc.* **1979**, *102*, 939–947.

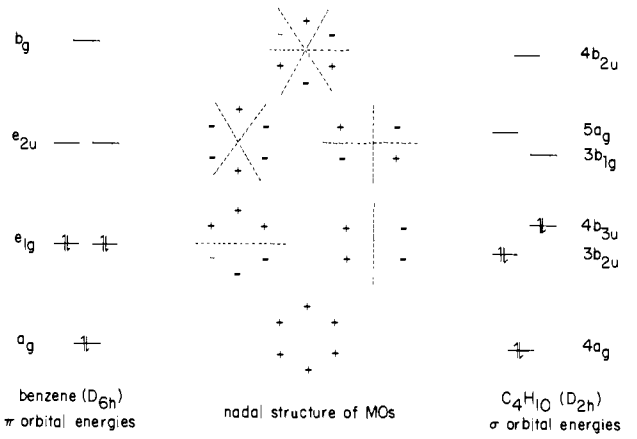

Figure 3. Comparison of the nodal structure of the reactive MO's of the transition state with that of the π-MO's of benzene.

to be $2183i$ cm^{-1}, indicating a rather sharply curved energy surface in the direction of the reaction coordinate. The latter is the b_{3u} normal mode which consists of the set of atomic displacements displayed in Figure 2. It is apparent that the left-hand side of this figure depicts the deformation toward ethane (decrease of the HCC angle, increase of the CC distance, decrease of the distance between carbon and its neighboring central hydrogen), whereas the right-hand side depicts the deformation toward ethylene (increase of the HCC angle, decrease of the CC distance, increase of the distance between carbon and its neighboring central hydrogen). The center of mass is of course at rest. If the central hydrogens are thought of as belonging to the right-hand part of the complex, then the indicated displacements describe the entrance of the reactants into the transition state. If the central hydrogens are imagined to belong to the left-hand part of the complex, then the picture describes the exit out of the transition state toward the products. Clearly this normal mode describes the *concerted* exchange of both hydrogens.

For ethylene the experimental geometry[18] was assumed, while for eclipsed ethane the SCF optimized geometry[19] was taken.

SCF Picture of the Electronic Structure. The low lying molecular orbitals which are *essentially* involved in this reaction arise from one sp^3-type hybrid on each carbon and a 1s-type orbital on each of the exchanging hydrogens. Each of these six orbitals contributes one electron to the reacting set. Because of the quasi-hexagonal arrangement of these atomic orbitals, the molecular orbitals of the activated complex are similar to those of the D_{6h} benzene π system. Of course, the hydrogen and carbon orbitals are inequivalent, lowering the symmetry to D_{2h} and lifting the degeneracy of the benzene e orbitals, as illustrated in Figure 3. Nonetheless the nodal structures of the transition-state orbitals are quite similar to those of benzene. For the SCF calculations the three lowest of these molecular orbitals are doubly occupied, and the three highest are vacant. This quasi-aromatic character of the transition state lends support to the view that the reaction is symmetry allowed. It should be noted, however, that the highest occupied orbital ($4b_{3u}$) in the activated complex is the π orbital of ethylene delocalized *antisymmetrically* between the left and right CC bonds and, hence, represents an *antibonding* combination of the left and right π MO's.

In addition to the three occupied MO's in the reaction zone which were just discussed, there are 14 additional occupied MO's corresponding to four carbon inner shells, two CC σ bonds, and eight peripheral CH bonds. When canonical SCF orbitals are determined, then the ten nonreacting valence MO's get mixed with the three occupied reaction MO's discussed in the preceding paragraph. In order to identify clearly the essential changes along the reaction path, it is therefore necessary to generate molecular orbitals that are localized inside and outside the reaction zone. We accomplished this separation into reacting and nonreacting

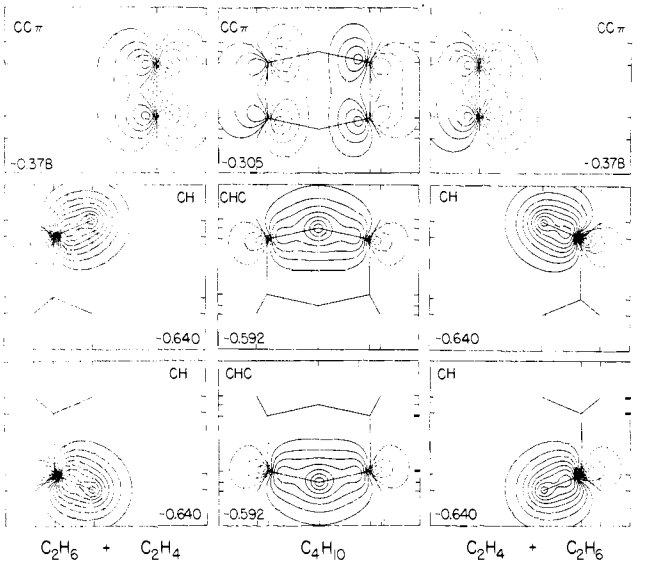

Figure 4. Partially localized SCF MO's in reaction zone (orbital symbols for reference to Figure 7; numerical values = orbital energies in hartrees). In this and all subsequent contour plots, the increment between any two consecutive contours is 0.05 bohr$^{-3/2}$.

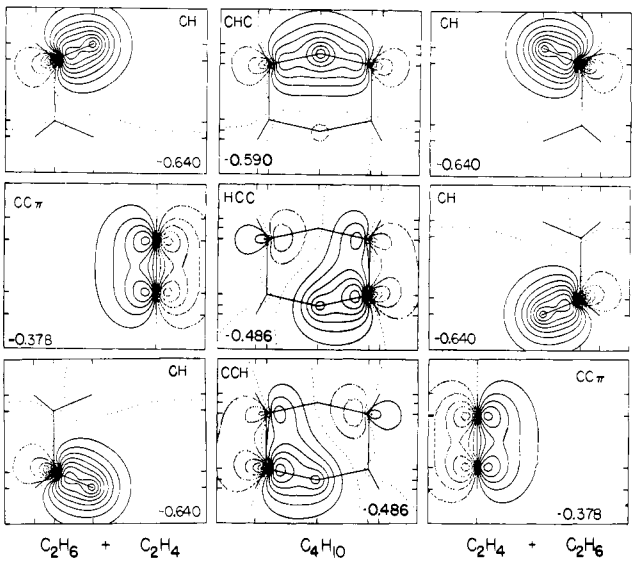

Figure 5. Completely localized SCF MO's in reaction zone (numerical values = orbital energies in hartrees).

MO's by performing the following partial Edmiston–Ruedenberg localization.[20] In ethane all valence MO's were localized, yielding one CC σ bond and six CH σ bonds. In ethylene the five σ valence MO's were localized, yielding one CC σ bond and four CH σ bonds, but the π MO was left in canonical form. For the activated complex, 12 MO's were localized, namely, all valence MO's excepting only the $4b_{3u}$ MO which was left in canonical form. This localization of the transition state yielded two equivalent CC σ bonds, eight equivalent peripheral CH σ bonds, and two equivalent CHC three-center bonds describing the concerted hydrogen transfer. The canonical $4b_{3u}$ MO describes the shift of the π bond from one CC atom pair to the other. Contour plots of the three reacting MO's mentioned last are shown in Figure 4 for the reactants/products and the transition state illustrating the progress of the reaction.

An alternative SCF MO interpretation of the transition state is obtained when *all* orbitals, *including* the $4b_{3u}$ MO, are incorporated in the localization process. When this is done one obtains, in the reaction zone, the MO's depicted in Figure 5 rather than those shown previously in Figure 4. (The SCF wave function

(18) Kuchitsu, K. *J. Chem. Phys.* **1966**, *44*, 906–911.
(19) Clementi, E.; Popkie, H. *J. Chem. Phys.* **1972**, *57*, 4870–4883.
(20) Edmiston, C.; Ruedenberg, K. *Rev. Mod. Phys.* **1963**, *35*, 457–465.

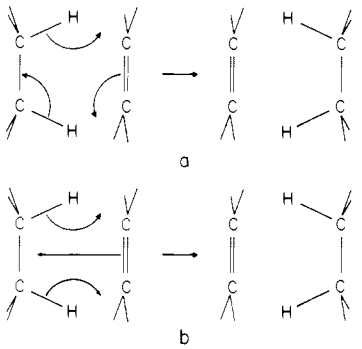

Figure 6. Schematic diagrams of orbital deformations corresponding to the intermediate stages illustrated in Figures 4 and 5. Diagrams a and b correspond to Figures 5 and 4, respectively.

Table II. Calculated Total Energies and Barrier to Dihydrogen Exchange

basis	level of calculation	C_4H_{10} (hartree)	C_2H_4 (hartree)	C_2H_6 (hartree)	barrier[a] (kcal/mol)
A	SCF	−156.6792	−77.8036	−78.9871	70.0
B	SCF	−157.0813	−78.0078	−79.1923	74.5
C	SCF	−157.1338	−78.0333	−79.2228	76.7
B	FORS	−157.1524	−78.0377	−79.2252	69.3

[a] Barrier equals $E(C_4H_{10}) - E(C_2H_4) - E(C_2H_6)$, where 1 hartree = 627.51 kcal/mol.

formed with the MO's of Figure 5 is of course identical with the one formed with the MO's of Figure 4.) The MO's of Figure 5 can be thought of as representing the intermediate stage of the continuous and concerted orbital shifts and deformations which are most easily summarized by the schematic diagram of Figure 6a. In the left column of Figure 5, the three MO's are localized into three two-center bonds. In the middle column, each one of them is delocalized into a three-center bond covering three adjacent atoms. In the right-hand column, each MO is now relocalized into the adjacent two-center bond. This picture of an MO "crawling" to a neighboring site corresponds remarkably well to the idea of "electron pushing" associated by organic chemists with shorthand diagrams such as Figure 6a. Figure 5 demonstrates that, for the reaction at hand, this type of diagram has a rigorous quantum mechanical meaning, if it is understood to imply adiabatic orbital deformations rather than dynamic motions of electrons.

Since the MO's depicted in Figure 4 provide a description of the transition state which is equally valid as that furnished by Figure 5, it is apparent that the electronic rearrangements can also be described by the continuous adiabatic orbital deformations that are implied by the schematic diagram of Figure 6b. In this description the $4b_{3u}$ MO, which represents the shift of the π bond, changes sign as it moves from right to left, as mentioned earlier. It is worth noting that, in the alternate description associated with Figure 5 and diagram 6a, an equivalent amount of antibonding character is embodied in the two MO's which are mixtures between a CH bond and a CC π bond (lower plots in Figure 5) in as much as they contain nonnegligible antibonding contributions on the C atoms diagonally across from the main orbital lobes.

Energies. SCF energies of ethylene, eclipsed ethane, and the intermediate complex for all three bases are reported in Table II, along with the predicted reaction barriers. These barriers are *underestimates* because of the assumption of an eclipsed conformation for ethane as it enters the reaction coordinate. Nontheless they are all quite large. The computed SCF reaction barrier increases with increasing flexibility of the basis to a value of nearly 77 kcal/mol for the largest bases considered.

That this barrier is related to the energetic changes of the three reacting MO's depicted in Figure 4 can be inferred from Figure 7. It exhibits quantitatively the orbital energies, i.e., the diagonal elements of the Fock matrix, of all σ-type localized valence orbitals and of the π canonical orbitals for the reactants/products and

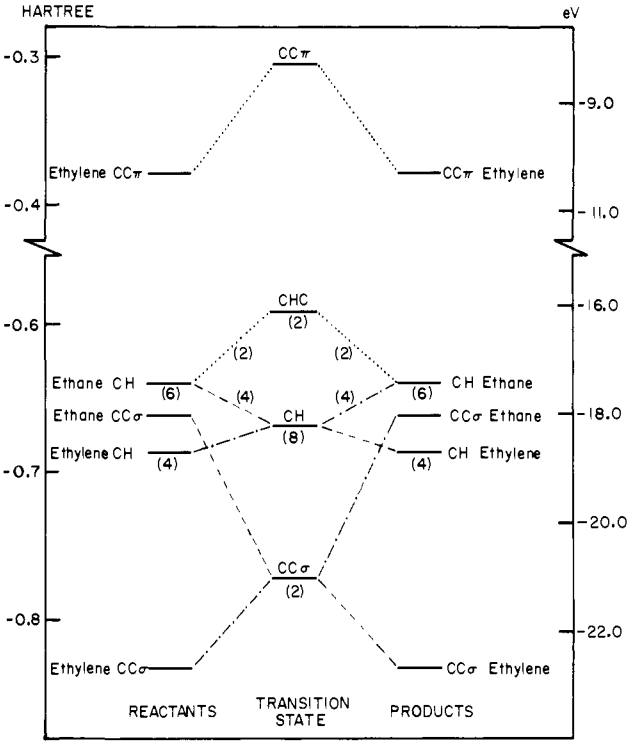

Figure 7. Orbital energies of SCF MO's localized in reaction zone for reactants/products and for transition state. Orbital symbols refer to Figure 4.

Table III. Breakdown of "Sum-of-Orbital-Energies Barrier" in Terms of Contributions from Various Orbital Types

orbital types of Figure 4	ΔE[a]	orbital types of Figure 5	ΔE[a]
4 carbon inner shells	+10.4	4 carbon inner shells	+10.4
2 CC σ bonds	−61.8	2 CC σ bonds	−61.8
8 peripheral CH bonds	−46.9	8 peripheral CH bonds	−46.9
2 reacting CH bonds	+120.4	1 reacting CH bond	+60.2
1 reacting CC π bond	+92.1	2 bonds changing from CH to CC π or vice versa	+152.3
total	114.2	total	114.2

[a] $\Sigma_n 2\epsilon_n(C_4H_{10}) - \Sigma_n 2\epsilon_n(C_2H_4) - \Sigma_n 2\epsilon_n(C_2H_6)$ expressed in kcal/mol.

for the transition state, the connecting lines indicating the progress of the reaction. It is apparent that the orbital energies of the ten nonreacting MO's vary smoothly from the (higher) ethane values to the (lower) ethylene values, with the transition state having intermediate values. By contrast the three MO's which are localized in the reaction region, i.e., the $4b_{3u}$ MO and the two CHC three-center MO's all have substantially higher values for the activated complex than for the reactants and products.

The numerical values of the MO energies of the reacting MO's are also indicated on Figure 4. The orbital energies of the alternate orbitals of Figure 5 are contained in Figure 5.

The invariant sum of *all* orbital energies is 114 kcal/mol higher for the transition state than for the reactants/products and, thus, of the same order of general magnitude as the actual barrier. (The sum of the SCF orbital energies is well-known to differ from the total SCF energy by the electron repulsion energy.) A breakdown of this 114 kcal/mol according to contributions from the various orbital types shown in Figures 4, 5, and 7 is given in Table III.

Results and Discussion of FORS Calculations

In view of the large barrier found in the SCF approximation, the following two questions arise. (i) Is this result significantly changed when the wave function allows for correlation? (ii) Is

the reaction in fact symmetry allowed? The dominant changes due to correlation are described by the FORS model which moreover provides further insight into the electronic rearrangements.

Wave Functions and Energies. The FORS wave function of the activated complex consists of the 42 A_g space orbital products, including the SCF configuration, which can be formed by distributing the six reacting electrons over the six reaction orbitals which are similar in shape to those indicated in Figure 3. All possible couplings of these space orbital products with the one or two permissible spin eigenfunctions yield a total of 52 ^1A_g SAAP's which comprise the configurational basis for the FORS function. In all of them the remaining 14 MO's are left doubly occupied (but not frozen) as the "nonreactive core". The optimization was performed as follows. Two preliminary six SAAP MCSCF calculations followed by CI calculations for configuration selection preceded the final eight SAAP MCSCF orbital optimization. A final CI calculations was performed to obtain the final FORS energy, wave function, and natural reaction orbitals.

The corresponding configurational FORS bases for the reactants/products are as follows. In ethylene it consists of the two singlet SAAP's of appropriate symmetry that can be made from the bonding π-MO and the antibonding π-MO. In ethane it consists of 12 singlet SAAP's of appropriate symmetry which are possible by using the bonding and antibonding σ-MO's in the two reactive CH bonds, the other four CH bonds and the CC σ bond remaining described by doubly occupied bonding MO's. The ethylene FORS wave function was obtained by direct MCSCF optimization, while a preliminary three SAAP MCSCF calculation preceded the final 12 SAAP MCSCF calculation on ethane. The FORS wave function of the reactant/product state is simply the normalized antisymmetrized product of the ethane and ethylene FORS wave functions and, hence, is a superposition of 24 SAAP's.

Only basis B was used for these calculations, and the FORS energies of all three molecules are presented as the final entry in Table II. Although for each molecule the FORS energy is much lower than the SCF energy using the same basis, the *difference* in the electron correlation energy of the reactants/products and the intermediate complex is merely 8.3 mhartree, corresponding to *a barrier lowering of only 5 kcal/mol.*

For the transition state as well as for the reactant/product state, the SCF-type configuration (in terms of natural orbitals) is dominant by far. In the 52-term transition-state FORS wave function this SAAP has the coefficient 0.967 corresponding to a weight of 92%. In ethane and ethylene the SCF-type SAAP's have the coefficients 0.9903 and 0.9767, respectively so that the coefficient of the SCF-type configuration in the 24-term FORS wave function of the reactant/product state is 0.9903 × 0.9767 = 0.967 as well. *It is therefore indeed justified to consider the reaction as symmetry allowed.*

FORS Picture of the Electronic Structure. As usual for any sensibly formulated FORS function, the physical interactions automatically localize the six reactive MO's in the reaction zone and the 14 (inner shell and valence) core MO's outside the reaction zone. The core MO's can be transformed among each other by an arbitrary orthogonal transformation, and the same holds true among the reactive MO's. Localization of the core MO's yields MO's that are very similar to the corresponding SCF MO's. In the orbital space of the six reactive orbitals, several choices of FORS MO sets are of interest.

The six *natural reaction orbitals* of the FORS wave functions for the three molecules, obtained by diagonalizing the first-order density matrix, are shown in Figure 8. They furnish the orbital description which is closest to the SCF orbital description, in that it has the smallest number of dominant FORS MO's. The nodal surfaces of the natural reaction orbitals of the transition state are very similar in both number and location to those of the schematic MO's which were conjectured in Figure 3. Each orbital deforms in a smooth and continuous fashion from reactants to activated complex to products, in accordance with the symmetry-allowed nature of the reaction. The symmetry-allowed nature is furthermore confirmed by the *near constancy of the electron occupations* of the nearly doubly occupied orbitals in Figure 8 and by the smallness of the occupation numbers of the correlating orbitals in Figure 8.

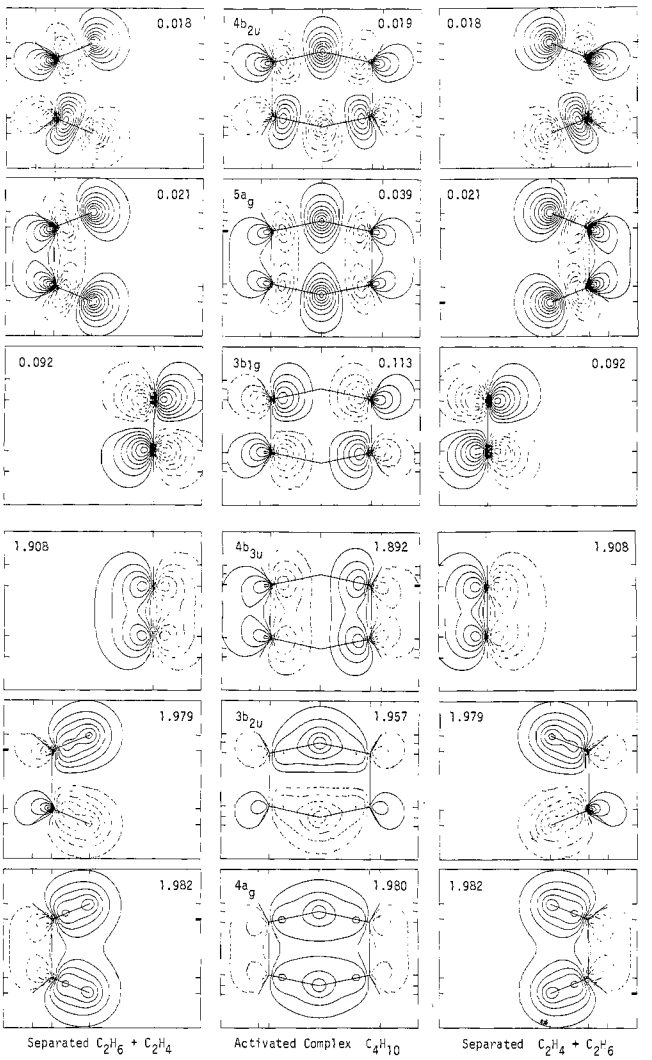

Figure 8. Natural reaction orbitals of FORS wave functions (numerical values = occupation numbers).

Localization of the six natural reaction orbitals according to the Edmiston–Ruedenberg energy criterion[20] yields the six AO-like molecular orbitals shown in Figure 9. These *localized reaction* orbitals have the somewhat deformed shapes of the hydrogen is AO's and the carbon hybrid AO's which were used conceptually to generate the symmetry-adapted full reaction space orbital set. The localized reaction orbitals represent "molecule-adapted minimal basis atomic orbitals". That is, the minimal basis set AO's can be imagined as having been deformed in such a fashion that they are directly useable as orthogonal FORS MO's. Conceptually, all other FORS MO's, such as e.g., the natural reaction orbitals, can then be conveniently thought of as being obtained from the localized reaction orbitals by orthogonal transformations. In this manner they can be easily visualized.

The localized reaction MO's of the FORS wave functions for ethane and ethylene have very similar shapes, and Table IV lists *all* populations and bond orders for the localized reaction orbitals of reactants, products, and the transition state. For the transition state the populations and bond orders between adjacent pairs are also indicated in Figure 9. The values of the bond orders are readily understood as the sum of the contributions made by the three dominant natural reaction orbitals shown in Figure 8, i.e., $p_{ij} \approx 2\sum_n T_{in}T_{jn}$, where n = $4a_g$, $3b_{2u}$, and $4b_{3u}$ and T is the transformation from natural to localized reaction orbitals. (For example, the substantial negative CC bond order diagonally across the ring results from the positive $4a_g$ contribution and the negative

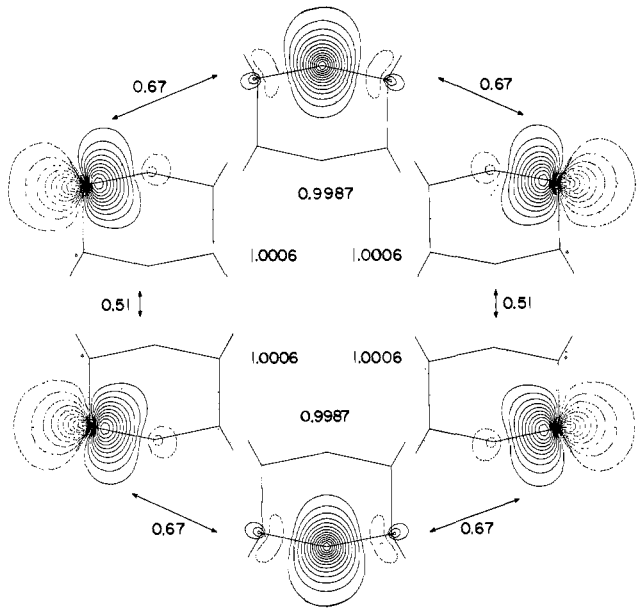

Figure 9. Localized reaction orbitals of FORS wave function at transition state (numerical values on the inside = orbital occupation numbers; numerical values between orbitals = bond orders).

Table IV. Populations and Bond Orders of Localized Reaction Orbitals

position	ethane	transition state	ethylene
	Populations		
C atom	1.0053	1.0006	1
H atom	0.9947	0.9987	0
	Bond Orders		
CH(neighbors)	0.9787	0.6798	0
CC(neighbors)	0.0610	0.5122	0.9081
CH(next neighbors)	−0.0003	0.0006	0
CC(next neighbors)	0	−0.0018	0
CC(third neighbors)	0	−0.3778	0
HH(third neighbors)	−0.0588	−0.1128	0

contributions from the $3b_{2u}$ and $4b_{3u}$ MO's.) From Table IV the following inferences can be drawn. (i) Each localized reaction orbital remains occupied by almost exactly one electron throughout the reaction. (ii) In ethane the two strong CH bonds interfere little with each other. (iii) The corresponding CH bonds in the transition state are weaker than those in ethane. (iv) The π bond between the neighboring carbons, too, is weaker in the transition state than in ethylene. (v) In the transition state, all CH bonds and CC bonds interact with each other. (vi) There is some antibonding character across the ring which presumably contributes to the barrier.

It should be noted that the occupation numbers and bond orders given in Figure 9 and in Table IV are the elements of the first-order density matrix in terms of the *orthogonal* MO's given in Figure 9 and, hence, are entirely unambiguous. In view of the strong localization of these orbitals these occupation numbers imply that, of the six reacting electrons, a charge of one resides near each of the six reacting atoms in the transition state. (These populations are not Mulliken populations, which refer to nonorthogonal and less localized atomic basis orbitals. In the present case, a Mulliken population analysis distributes the six reacting electrons as follows: reacting hydrogen = 0.930; carbon = 1.020; and peripheral hydrogen = 0.007. In view of the well-known questions regarding the definition of Mulliken populations, the meaning of these values is less definite.)

Further sets of interesting FORS MO's are *chemically adapted reaction orbitals*, which we define as MO's that have *nearly* maximal or minimal occupation numbers and, *in addition*, are also localized in as small a part of the molecule as possible. For the transition state, a chemically adapted reaction orbital set is given in Table V in terms of the localized reaction orbitals. It is readily seen that three of these MO's have occupation numbers close to 2 and are very similar in shape to the partially localized SCF MO's, which were depicted in Figure 4. Each of the remaining three MO's is seen to be an orbital which essentially provides "interatomic" electron correlation to *one* of the three dominant MO's. Another set of chemically adapted reaction orbitals is given by the orthogonal transformation in Table VI. It is readily verified that those MO's with occupation numbers close to 2 are very similar to the completely localized SCF MO's of Figure 5 and that each of those MO's with near-zero occupation numbers again provides interatomic correlation to one of the dominant MO's. From the expansions in this table, the antibonding character across the ring mentioned earlier for the MO's |CCH) and |HCC) is particularly evident.

Table V. Chemically Adapted Reaction Orbitals Corresponding to SCF MO's of Figure 4 in Terms of Localized Reaction Orbitals[a]

	$\|C_1>$	$\|H_1>$	$\|C_2>$	$\|C_3>$	$\|H_2>$	$\|C_4>$	occupation nos
$\|CHC>_1$	$1/2$	$1/2\sqrt{2}$	$1/2$	0	0	0	1.961
$\|CHC^*>_1$	$1/2$	$-1/2\sqrt{2}$	$1/2$	0	0	0	0.039
$\|CHC>_2$	0	0	0	$1/2$	$1/2\sqrt{2}$	$1/2$	1.961
$\|CHC^*>_2$	0	0	0	$1/2$	$-1/2\sqrt{2}$	$1/2$	0.039
$\|CC\pi>$	$1/2$	0	$-1/2$	$-1/2$	0	$1/2$	1.890
$\|CC\pi^*>$	$1/2$	0	$-1/2$	$1/2$	0	$-1/2$	0.110

[a] Column headings: localized reaction orbitals, as shown in Figure 7, corresponding to the indicated atoms (progressing counterclockwise, starting at the 1 o-clock position). Row headings: chemically adapted reaction orbitals (labels have meanings similar to those used in Figure 4).

Table VI. Chemically Adapted Reaction Orbitals Corresponding to SCF MO's of Figure 5 in Terms of Localized Reaction Orbitals

	$\|C_1>$	$\|H_1>$	$\|C_2>$	$\|C_3>$	$\|H_2>$	$\|C_4>$	occupation nos
$\|CHC>_1$	$1/2$	$1/2\sqrt{2}$	$1/2$	0	0	0	1.961
$\|CHC^*>_1$	$1/2$	$-1/2\sqrt{2}$	$1/2$	0	0	0	0.039
$\|HCC>$	$1/4\sqrt{2}$	0	$-1/4\sqrt{2}$	0	$1/2$	$1/2\sqrt{2}$	1.925
$\|HCC^*>$	$-1/4\sqrt{2}$	0	$1/4\sqrt{2}$	0	$-1/2$	$1/2\sqrt{2}$	0.075
$\|CCH>$	$-1/4\sqrt{2}$	0	$1/4\sqrt{2}$	$1/2\sqrt{2}$	$1/2$	0	1.925
$\|CCH^*>$	$1/4\sqrt{2}$	0	$-1/4\sqrt{2}$	$1/2\sqrt{2}$	$-1/2$	0	0.075

[a] Labellings similar to those in Table V.

Discussion of Barrier

The calculated zero-point vibrational energies of ethylene, eclipsed ethane, and the activated complex are 0.0547, 0.0787, and 0.1318 hartree, respectively. Thus, the inclusion of zero point vibrational energies lowers the barrier by 0.0016 hartree, which is just 1.0 kcal/mol.

On the basis of these calculations, the reaction barrier is estimated to be 71 kcal/mol. This estimate is obtained by subtracting the 5-kcal/mol lowering due to the inclusion of electron correlation, using basis B, and the 1-kcal/mol lowering due to the inclusion of the zero-point vibrational energy, from the SCF barrier of 77 kcal/mol obtained by using basis C. Further calculational improvements are unlikely to lower the barrier significantly, as the largest basis used is quite flexible, and the FORS method can be expected to incorporate the pertinent changes in electron correlation which occur during the course of a reaction. Taking into account the rotational barrier in ethane, we finally infer a dihydrogen exchange barrier of about 74 kcal/mol between staggered ethane and ethylene.

The origin of this large barrier is apparent from Figures 7 and 8. *While the symmetry allowedness ensures that the occupancies of the three frontier MO's remain close to 2 along the entire reaction path, it does not prevent the energies of these orbitals from changing drastically.* In fact, all three have significantly

Table VII. Orbital Energies of SCF MO's Corresponding to the Natural FORS MO's of Figure 8

orbital	ethane/ ethylene	activated complex	ethylene/ ethane
S(π), $4b_{3u}$	−0.378	−0.305	−0.378
A(CH), $3b_{2u}$	−0.604	−0.506	−0.604
S(CH), $4a_g$	−0.677	−0.679	−0.677

higher orbital energies for the reaction intermediate than for the reactants/products. The energy increase contributed by the CHC bonds is associated with the fact that the two-electron, two-center CH bonds of ethane become CHC two-electron, three-center bonds, a circumstance which dilutes and weakens the binding effect and, thereby, leads to a considerable elongation of the CH bonds with a concomitant rise in energy. For very similar reasons, the spread of the two-electron, two-center π bond of ethylene over both CC bonds dilutes and weakens the bonding effect of the π electrons, as evidenced by the lengthening of the CC bonds compared to ethylene. In addition, the CC π bond is further destabilized by the left–right antisymmetry of the $4b_{3u}$ MO which creates an antibinding effect that increases with decreasing distance between the reactants.

For the purpose of comparing the present results with the schematic Figure 40 of Woodward and Hoffman,[1a] we finally formed the normalized sum and difference of the two localized CHC three-center SCF MO's of the transition state and the same linear combinations of the two corresponding CH localized SCF MO's in ethane. (Plots of the localized MO's were shown in Figure 4.) The resulting SCF MO's have shapes which are very similar to the natural reaction orbitals $4a_g$ and $3b_{2u}$ and the corresponding ethane orbitals shown in Figure 8. The energies of these SCF MO's are given in Table VII for the reactants/products and the transition state. In this formulation the barrier contributions from the CHC three-center bonds are seen to be entirely concentrated in the orbital which is antisymmetric with respect to the CC bond bisectrix, whereas the symmetric orbital has nearly the same energy in the transition state as in ethane. This is so because the off-diagonal Fock matrix element between the two localized CHC MO's of the transition state is much larger than the corresponding matrix element between the CH bonds in ethane. This increase in the interference energy between the two localized CHC MO's is probably due to the shortening of the CC distances and of the distance between the central hydrogens. The orbitals $4a_g$, $3b_{2u}$, and $4b_{3u}$ correspond conceptually to the orbitals denoted by S(CH), A(CH), and S(π) in Figure 40 of ref 1a.

Since the D_{2h} transition state has such a high energy, one might finally raise the question whether there exists a nonplanar transition state, similar to the chair or boat form of cyclohexane, whose saddle point is lower than the one considered here. While we have not made an exhaustive study of all possible geometries, we have investigated the variation of the energy for the following deformations of the planar arrangement. The four carbon atoms were kept in a plane, all distances between neighbor atoms were kept at their transition state values, and all bond angles at the *carbon* atoms were held fixed as well. These constraints restrict the motions of the hydrogen atoms to rigid cylindrical rotations around the left and right CC bonds, respectively, so that the bridge hydrogens are limited to one-dimensional out-of-plane motions and the distance between the left and right CC bonds decreases somewhat. The maximum displacements considered were approximately those where the angle between the CCCC plane and the bonds to the bridge hydrogens were equal to the corresponding angles in cyclohexane, at which point the distance between the left and right CC bonds is shortened by about 0.15 Å only. The boat form as well as chair form was investigated. Specific geometric parameters and the corresponding changes in the SCF energy are listed in Table VIII. In view of the strong increase of the energy relative to the D_{2h} transition state, it seems unlikely that there exists another saddle point describing a concerted hydrogen exchange. The reason for this energetic behavior must

Table VIII. Energies of Activated Complex for Out-of-Plane Deformations of Transition-State Geometry

geometric data				energies	
Z_B[a]	θ_B[b]	C_1C_2[c]	H_pH_p[d]	ΔE- (chair)[e]	ΔE- (boat)[e]
0	0	2.704	3.276	0	0
±0.1	10.55	2.702	3.201	0.33	0.16
±0.3	29.19	2.685	3.038	2.98	1.46
±0.6	48.17	2.628	2.754	12.68	6.08
±0.9	59.18[f]	2.531	2.421	31.88	15.20

[a] Components of bridge hydrogen positions perpendicular to CCCC plane in bohrs (coordinate system in Figure 1). [b] Dihedral angle between CCCC plane and CH_BC planes in degrees (H_B = bridge hydrogens). [c] Shortest CC distance across the ring, between left and right C_2H_4 fragments, in angstroms. [d] Shortest HH distance between left and right peripheral hydrogens, in angstroms. [e] ΔE = (SCF energy of indicated geometry) − (SCF energy of D_{2h} transition state) in kcal/mol, calculated with 3-21G basis.[17] [f] Note: for cyclohexane one has $\theta_B = 54.74°$.

be seen in the difference between the electronic structure of this activated complex and that of cyclohexane. Whereas the ring in cyclohexane is formed by 12 electrons using six bonding MO's formed from 12 molecule adapted minimal basis set AO's, the ring in the transition state at hand is formed by 10 electrons using five bonding MO's formed from 10 molecule adapted minimal basis set orbitals. There exists thus an essential delocalization of at least two electrons over all four carbons. It seems therefore unlikely that the CHC bridge bonds can be significantly shortened and that the antibonding effect embodied in the $4b_{3u}$ MO will disappear when the ring is made nonplanar. It rather seems likely that matters will get worse, because the π-bonding character embodied *within* the left and right halves of the $4b_{3u}$ MO will be lost when both halves of the transition state assume the staggered conformation appropriate to the chair or boat form.

Conclusions

The results reported here for the prototype concerted dihydrogen exchange between ethane and ethylene imply that the *intrinsic* barrier (i.e., the barrier in the absence of other factors such as discussed below) for the dihydrogen exchange between alkyl and alkenyl carbons is about 71 (74) kcal/mol. This is surprisingly large and shows that neither the symmetry-allowed nature of the reaction nor the aromatic character of the transition state in themselves are sufficient to guarantee a low activation energy. The implication is that additional factors which stabilize the transition state are required to reduce the activation energy for dihydrogen exchange to a surmountable magnitude.

An example where such is the case is the analogous reaction between diimide and olefins,[4-6] where the formation of N_2 leads to a very large lowering in the energy of the products which, in turn, is expected to depress the activation energy substantially. Thus, we have for instance

$$N_2H_2 + C_2H_4 \rightarrow N_2 + C_2H_6 + \text{about 90 kcal/mol}$$

where N_2H_2 is assumed to be in the cis form. Pasto and Chipman[21] have calculated the barrier for this reaction to be about 27 kcal/mol. We view their result as a confirmation of the results obtained in the present investigation in the following sense. Even with the assistance of a very large heat of formation of the products there still survives a barrier as high as 27 kcal/mol.

Another example is the dihydrogen transfer from *cis*-9,10-dihydronaphthalene to olefins. With respect to this reaction our results lead us to agree with the comment by Doering and Rosenthal,[3] viz., "as the driving force in the hydrogenation by diimide is very probably associated with the contribution of the heat of formation of nitrogen to the transition state, so the driving force in the transfer of hydrogen from *cis*-9,10-dihydronaphthalene may be dependent on the unique possibility of contributing a part of

(21) Pasto, D. J.; Chipman, D. M. *J. Am. Chem. Soc.* **1979**, *101*, 2290–2296.

the full resonance energy of naphthalene (61 kcal/mol) to the transition state".

The intrinsic activation energy for the $[\pi_{2s} + \sigma_{2s} + \sigma_{2s}]$ concerted dihydrogen exchange appears to be very high and one is left to wonder whether there may exist a nonconcerted pathway with a lower activation energy.

The reaction discussed here is not the only case where a Woodward–Hoffman-allowed reaction has in fact a high activation energy. For instance, Feller et al.[22] have recently found calculated barriers of 30 and 50 kcal/mol for two other "allowed" concerted pericyclic shifts of three reactive electron pairs, namely, the decompositions of dihydroxycarbene and 2-carbena-1,3-dioxolane.

Acknowledgment. We wish to express our thanks to Dr. Stephen Elbert, whose constant improvements to the ALIS program system made these calculations feasible. We also extend our thanks to Professor Richard P. Johnson for a critical reading of the manuscript and very valuable comments. The vibrational analysis calculations were performed on the Chemistry Department VAX computer at the University of Washington. The present work was supported by the U.S. Department of Energy, Director of Energy Research, Office of Basic Energy Science, under Contract No. W-7405-Eng-82.

Registry No. Ethane, 74-84-0; ethylene, 74-85-1.

(22) Feller, D.; Borden, W. T.; Davidson, E. R. *J. Comput. Chem.* **1980**, *1*, 158–166. Feller, D.; Davidson, E. R.; Borden, W. T. *J. Am. Chem. Soc.* **1981**, *103*, 2558–2560.

Potential Surface for the Methylenecyclopropane Rearrangement

David Feller, Kiyoshi Tanaka, Ernest R. Davidson,* and Weston Thatcher Borden*

Contribution from the Department of Chemistry, University of Washington, Seattle, Washington 98195. *Received August 13, 1981*

Abstract: MCSCF calculations with an STO-3G basis set have been carried out to obtain the optimal geometries and associated energies for a grid of points on the lowest singlet potential surface connecting methylenecyclopropane (MCP) and trimethylenemethane (TMM). Two methylene rotation angles were used to generate a two-dimensional projection of the 24-dimensional hypersurface, and a double Fourier fit to the computed energies gave a closed form expression for the energy on the two-dimensional surface. Three minima, connected by four transition states, were located on the surface. The effect of basis set expansion and inclusion of CI on the relative energies was determined. In accord with Hammond's postulate, the energies of transition states leading to orthogonal and planar TMM were found to be in the same order as the energies of these two intermediates. The conrotary transition state leading to planar TMM was found to be slightly lower in energy than the disrotary one. From a Fourier fit to the triplet energies, calculated at the optimal singlet geometries on the two-dimensional surface, the line along which the singlet and triplet surfaces intersect has been found. The lowest point along this line was computed to be higher in energy than orthogonal TMM. The implications of this finding are discussed.

The thermal rearrangements of methylenecyclopropane (MCP) derivatives have been the subject of numerous experimental investigations.[1] These studies suggest that the major pathway involves the orthogonal geometry (**1**) in which one methylene group

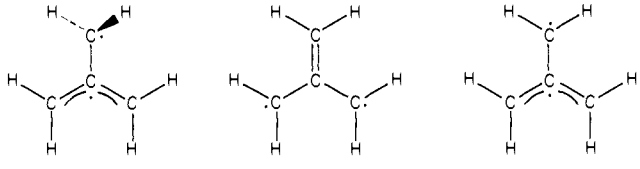

1 ($^1B_1$) 2a ($^1A_1$) 2b ($^1B_2$)

is twisted 90° out of conjugation with the rest of the π system.[2-7] However, a small amount of planar (**2**) trimethylenemethane (TMM) is apparently also formed.[8-10]

The preference for **1** over **2** in the lowest singlet state contrasts with the geometry of the lowest triplet state. Both the null value of the zero field splitting parameter E[11] and the hyperfine coupling pattern[12] suggest a triplet geometry of at least C_3 symmetry. Ab initio calculations predict the triplet geometry to be planar D_{3h}.[13] The difference between the preferred geometry of the singlet and triplet has been rationalized in terms of electron repulsion effects.[14]

A large number of calculations have been carried out to determine the relative energies of the planar and orthogonal singlet states, and all predict that the orthogonal singlet is lower.[15-23]

(1) Gajewski, J. J. "Hydrocarbon Thermal Isomerizations"; Academic Press: New York, 1981.
(2) Ullman, E. F. *J. Am. Chem. Soc.* **1960**, *82*, 505.
(3) Gajewski, J. J. *J. Am. Chem. Soc.* **1971**, *93*, 4450.
(4) Doering, W. von E.; Roth, H. D. *Tetrahedron* **1970**, *26*, 2825.
(5) Doering, W. von E.; Birladeanu, L. *Tetrahedron* **1973**, *29*, 449.
(6) Gilbert, J. C.; Butler, J. R. *J. Am. Chem. Soc.* **1970**, *92*, 449.
(7) Jones, M.; Hendrick, M. E.; Gilbert, J. C.; Butler, J. R. *Tetrahedron Lett.* **1970**, 845.
(8) Buchwalter, S. G. Ph.D. Thesis, Harvard 1974; *Diss. Abstr. Int. B* **1974**, *35*, 1564.
(9) Roth, W.; Wegener, G. *Angew. Chem., Int. Ed. Engl.* **1975**, *14*, 758.
(10) Gajewski, J. J.; Chou, S. K. *J. Am. Chem. Soc.* **1977**, *99*, 5696.
(11) Dowd, P. *J. Am. Chem. Soc.* **1966**, *88*, 2587.
(12) Dowd, P.; Gold, A.; Sachdev, K. *J. Am. Chem. Soc.* **1968**, *90*, 2715.
(13) Hood, D. M.; Pitzer, R. M.; Schaefer, H. F.; III *J. Am. Chem. Soc.* **1978**, *100*, 2227.
(14) Borden, W. T.; Salem, L. *J. Am. Chem. Soc.* **1973**, *95*, 932.
(15) Dewar, M. J. S.; Wasson, J. S. *J. Am. Chem. Soc.* **1971**, *93*, 3081.
(16) Hehre, W. J.; Salem, L.; Willcott, M. R. *J. Am. Chem. Soc.* **1974**, *96*, 4328.
(17) Yarkony, D. R.; Schaefer, H. F., III *J. Am. Chem. Soc.* **1974**, *96*, 3754.
(18) Davidson, E. R.; Borden, W. T. *J. Chem. Phys.* **1976**, *64*, 663.

0002-7863/82/1504-0967$01.25/0 © 1982 American Chemical Society